J. Mol. Model. **1997**, *3*, 455 – 463

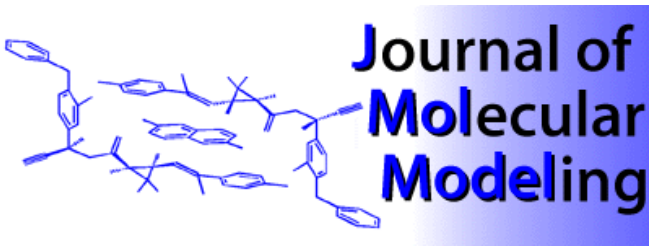

Three-dimensional Pharmacophore Hypotheses for the Locust Neuronal Octopamine Receptor (OAR3): 1. Antagonists

Canping Pan[1], Akinori Hirashima[1,*], Eiichi Kuwano[1], and Morifusa Eto[2]

[1] Department of Agricultural Chemistry, Kyushu University 46-02, Japan 812-81 (ahirasim@agr.kyushu-u.ac.jp)

[2] Miyakonojo National College of Technology, 473-1 Yoshio-cho, Miyakonojo 885, Japan

Received: 12 July 1997 / Accepted: 30 October 1997 / Published: 7 November 1997

Abstract

Three-dimensional pharmacophore hypotheses were built from a set of 17 mianserin-like antagonists against octopamine receptor class 3 (OAR3) in locust nervous tissue. Among the ten chemical-featured models generated by program Catalyst/Hypo, three hypotheses were considered to be important and predictive in evaluating OAR3 antagonists. Predictions were fairly precise for all molecules but the three outliners including eresepine, metoclopramide and yohimbine. While the ideal and null hypotheses had a cost of 66.50 and 124.97, respectively, the ten resulting hypotheses possessed costs from 78.96 to 92.04. The best hypothesis that was confirmed to have a 95% chance of true correlation yielded a low RMS of 1.05 and high regression *r* of 0.934. Active antagonists mapped well onto all the features of the hypothesis such as hydrophobic, aromatic ring or positive ionizable features. On the other hand, inactive compounds lack of binding affinity were shown to be poorly capable of achieving an energetically favorable conformation shared by the active molecules in order to fit the 3D chemical feature pharmacophore models. In addition, from the comparison and conformation analysis it was proposed that positive ionizable feature contained a lower weight than hydrophobic or an aromatic ring one. Further research on the comparison of models from agonists and antagonists may help elucidate the mechanisms of OAR3 and other types of octopamine receptor-ligand interactions.

Keywords: Octopamine, Antagonist, Receptor hypothesis, Pharmacophore, Locust

Introduction

In rational drug design process, it's the common situation that the binding activity data of a set of compounds acting upon a particular protein is known, while information of the three-dimensional structure of the protein active site is absent. Either a quantitative structure-activity (or structure-property) relationship model (QSAR/QSPR) or a three-dimensional pharmacophore hypothesis that is consistent with known data should be useful and predictive in evaluating new compounds and directing further synthesis. The QSAR/QSPR study assumes that the difference of the molecules in the structural properties experimentally measured or computed accounts for the difference in their observed biological or chemical properties [1-3]. The result of QSAR (QSPR) usually reflects as a predictive formula, while a pharmacophore model postulates that there is an essential three-dimensional

* *To whom correspondence should be addressed*

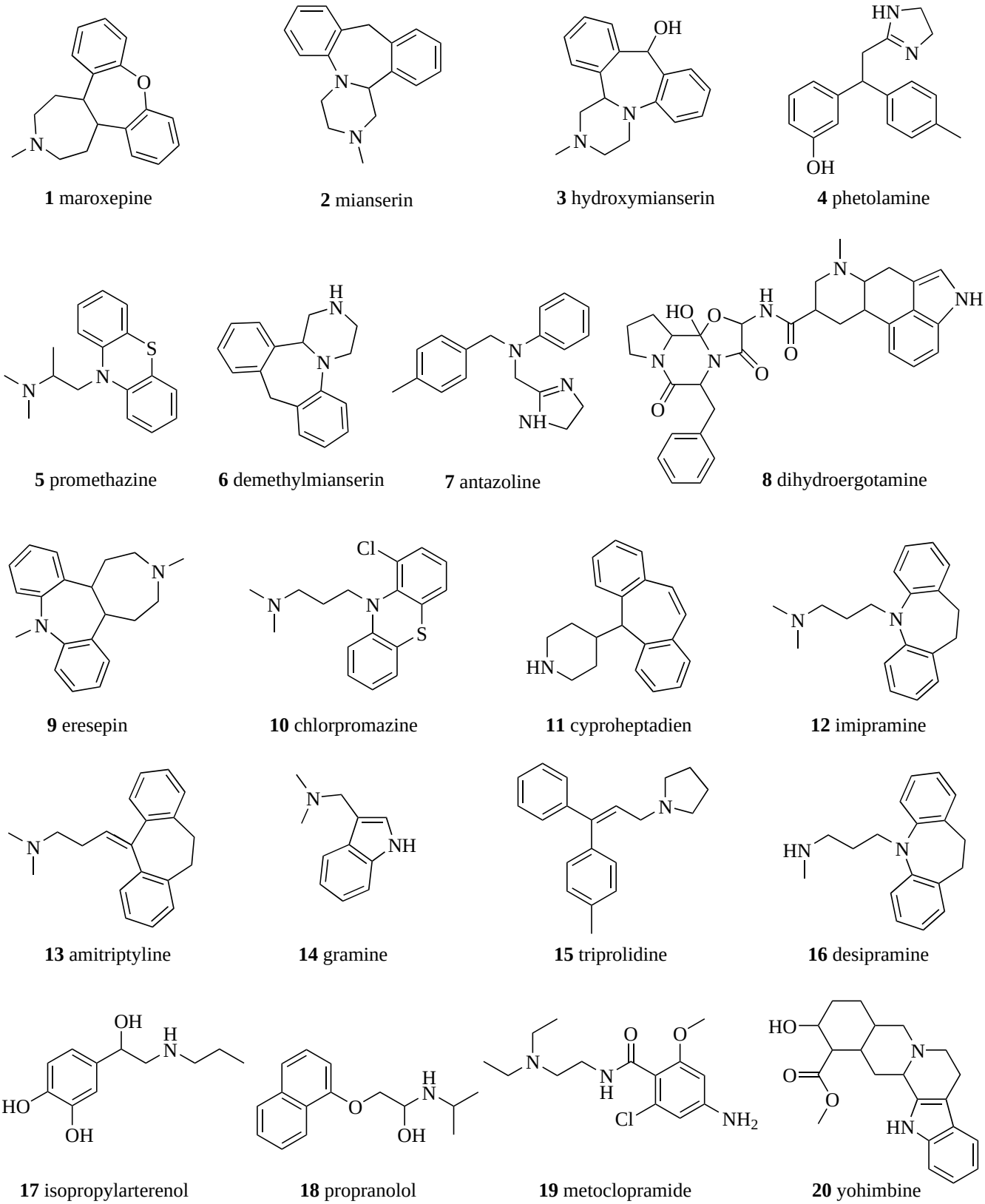

Figure 1. *Structures of octopamine antagonists in the training and test set.*

arrangement of functional groups that a molecule must possess to be recognized by the receptor. It collects chemical features distributed in 3D space that is intended to represent groups in a molecule that participates in important binding interactions between ligands and their receptors. Hence, a pharmacophore model provides both crucial information about how well the chemical features of a subject molecule overlap with the hypothesis model and the ability of molecules to adjust their conformations in order to fit a receptor with energetically reasonable conformations. Such characterized 3D models convey important information in an intuitive manner and can provide predictive capability for evaluating new compounds.

Octopamine receptors are perhaps the only non-peptide receptors whose occurrence is restricted to invertebrates. Recently much attention has been directed at the octopaminergic system as a valid target in the development of safer and selective pesticides [4]. The biogenic monoamine octopamine (*p*-hydroxyethanolamine), which is the monohydroxylic analogue of the vertebrate hormone noradrenaline, was first discovered in the salivary glands of octopus by Erspamer and Boretti in 1951 [5]. It's found that octopamine is present in a high concentration in various invertebrate tissues [6]. This multifunctional and naturally occurring biogenic amine has been well studied and established as 1) a neurotransmitter, controlling the firefly light organ and endocrine gland activity in other insects; 2) a neurohormone, inducing mobilization of lipids and carbohydrates; 3) a neuromodulator, acting peripherally on different muscles, fat body and sensory organs such as corpora cardiaca and the corpora allata and 4) a centrally acting neuromodu-lator, influencing motor patterns, habituation and even memory in various invertebrate species [7-9]. The action of octopamine is mediated through various receptor classes which is coupled to G-proteins and is specifically linked to an adenylate cyclase. Thus, the physiological actions of octopamine have been shown to be associated with elevated levels of cyclic AMP [10]. Three different receptor classes OAR1, OAR2A, and OAR2B had been distinguished from non-neuronal tissues [11]. In the nervous system of locust, a particular receptor class was characterized and established as a new class OAR3 by pharmacological investigations of the [^{3}H]-octopamine binding site using various agonists and antagonists.

Our interest in octopaminergic antagonists was aroused by the results of QSAR study using molecular similarity indexes from rigid or flexible fitting as descriptors (unpublished data). It was found that electrostatic and atom matching indices gave reasonable regressions exemplified by Eq. 1 (log P is the standard physicochemical parameter calculated by atom-type scheme, Rfe. stands for the electrostatic similarity index from rigid fitting.)

$$pK_i = 0.673\log P + 142.903Rfe \quad (1)$$

[n=20, SD=1.22, R=0.62, F(2,17)=5.39]

Until now, no 3D structure-activity model has been reported in these ligand-receptor interactions. Eq. 1 was improved by excluding 3 outliners and regressing again, which was proved to be useful in conformational analysis and appears to be a good predictive model. Furthermore, molecular modeling and conformational analysis were performed in Catalyst/Hypo to gain a better knowledge of the interactions between octopaminergic compounds and OAR3, in order to understand identification of the conformations required for binding activity. The current work is aimed to generate 3D chemical function-based hypotheses from some set of octopamine antagonists, in which were tested the [^{3}H]-octopamine binding to OAR3 in the locust central nervous tissue.

Methods and Experimental

Antagonists and their bioassay activities

Twenty molecules that employ a single [^{3}H]octopamine binding criteria were selected from recent publications by Roeder T. [12-14]. The respective IC_{50} values of the antagonists had been corrected according to the Cheng-Prusof correction [$K_i = IC_{50}/(1+ K/K_d)$] in order to obtain the K_i values. The antagonists especially those which share structural homologies with mianserin have been investigated. Their chemical structures and experimental activities are listed in Fig. 1 and Table 2.

Catalyst/Hypo methodology

Set of compounds: In using a "garbage in garbage out" strategy, metoclopramide (**19**, 52,480 nM), yohimbine (**20**, 81,283 nM) and eresepine (**9**, 478.6 nM) couldn't be understood by Catalyst. According to the rules of Catalyst/Hypo (according to on-line manual of Catlalyst), these three outliners were considered to be unsuitable for generating hypothesis and statistical analysis. Molecules **19** and **20** may be considered to have volume problems. In other words, these molecules have the functionality that bumps into a portion of the receptor preventing close contacts of the binding functions. Compound **9** might also contain some unknown negative features. In another point of view, as Catalyst pays particular attention to the most active compounds in the training set, excluding such inactive compounds as **19** and **20** may not generally affect the generation of the chemical feature space relevant to the experiment. And as the order of magnitude including **9** contains other four molecules, **9** was dropped out so that each compound in the training set possesses something new to teach Catalyst. Thus, a set of 17 molecules that employs a single [^{3}H]octopamine binding criteria was selected from the reported data as the target training set. Affinities of the antagonists are expressed as their pK_i values in nanomole and activities range over four orders of magnitude (min. 1.02 nM and max. 29,500 nM).

Table 1. *Characteristics of ten lowest cost hypotheses from 17 OAR3 antagonists (cost of ideal hypothesis: 66.50, cost of null hypothesis: 124.97)*

Hypotheses	Function1	Function2	Function3	Cost	RMS	*r*
1	Hp 1	Hp 2	RA	78.96	1.047	0.934
2	Hp 1	Hp 2	RA	79.11	1.102	0.924
3	Hp	RA 1	RA 2	79.47	1.093	0.927
4	Hp	RA 1	RA 2	79.68	1.129	0.920
5	Hp	RA 1	RA 2	80.44	1.151	0.918
6	Hp 1	Hp 2	RA	83.12	1.330	0.885
7	Hp	RA 1	RA 2	85.83	1.424	0.868
8	PI	RA 1	RA 2	88.05	1.461	0.864
9	PI	RA 1	RA 2	88.12	1.493	0.885
10	PI	RA 1	RA 2	92.04	1.668	0.811

Abbreviations: Hp hydrophobic; RA ring aromatic; PI positive ionizable.

Molecular modeling: energy minimizing and conformation search: Molecules were created using CAChe Editor (version 3.8), followed by energy minimization from molecular mechanics (MM2) and MOPAC (AM1, PM3) (Details were given previously [15]). After importing the MOL files transferred by CAChe translator, Catalyst automatically generated no more than 255 conformational models for each compound using the Poling Algorithm. The models emphasized a conformational diversity under the constraint of 20 kcal/mol energy threshold above the estimated global minimum based on use of the CHARMm force field [16,17].

Hypothesis generation and validation: The above molecules associated with their conformational models was submitted to Catalyst hypothesis generation. This process only considered surface accessible functions such as hydrogen bond acceptor, hydrogen bond donor, hydrophobic, negative charge, positive charge and ring aromatic *etc*. The hypothesis generator was restricted to select only five features due to the molecule's flexibility and functional complexibility. A preparative test was performed with hydrogen bond acceptor (HBA), hydrogen bond donor (HBD), hydrophobic (Hp), negative ionizable (NI) and positive ionizable (PI). NI and PI were used rather than negative charge and positive charge in order to broaden the search for deprotonated and protonated atoms or groups at physiological pH. It was found that hypotheses contain good correlation with HBA, Hp and PI. Furthermore, in order to emphasize the importance of an aromatic group corresponding to the phenol moiety of octopamine, ring aromatic (RA) which consists of directionality was chosen to be included in the subsequent run.

During a hypothesis generation run, Catalyst considers and discards many thousands of models. It attempts to minimize a cost function consisting of two terms. One penalizes the deviation between the estimated activities of the training set molecules and their experimental values. The other penalizes the complexity of the hypothesis. The overall assumption used is based on Occam's razor, that between otherwise equivalent alternatives, the simplest model is best. Simplic-

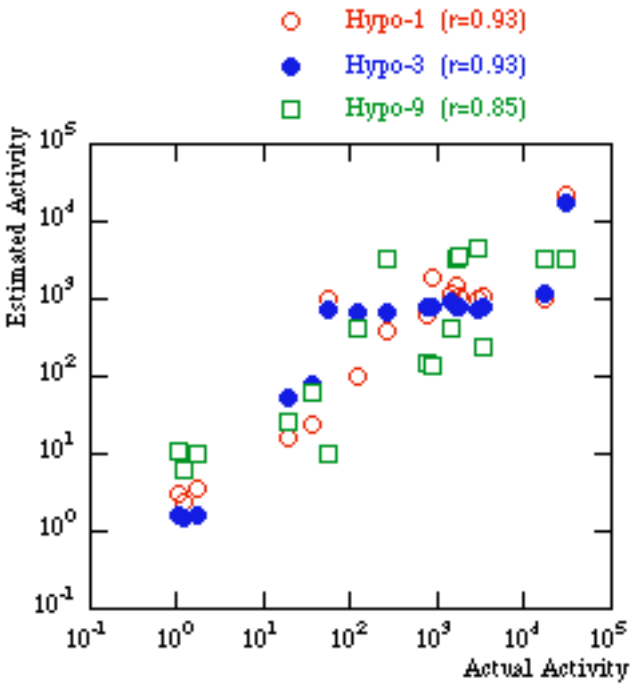

Figure 2. *Plot of predicted binding affinity activities against experimental values* (pK_i *in nM).*

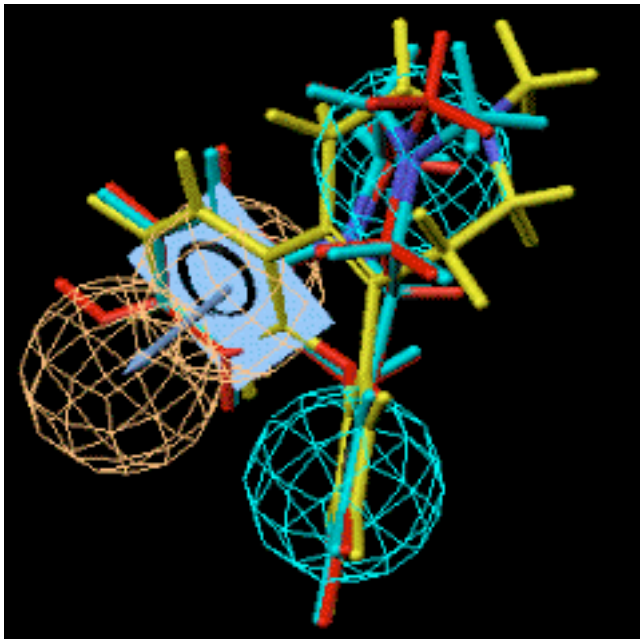

Figure 3a. *Mapping of mianserin (light green), hydroxymianserin (red) and maroxepine (yellow) onto hypotheses* ***1,*** *which contains hydrophobic 1 (green), hydrophobic 2 (green) and ring aromatic (yellow) features.*

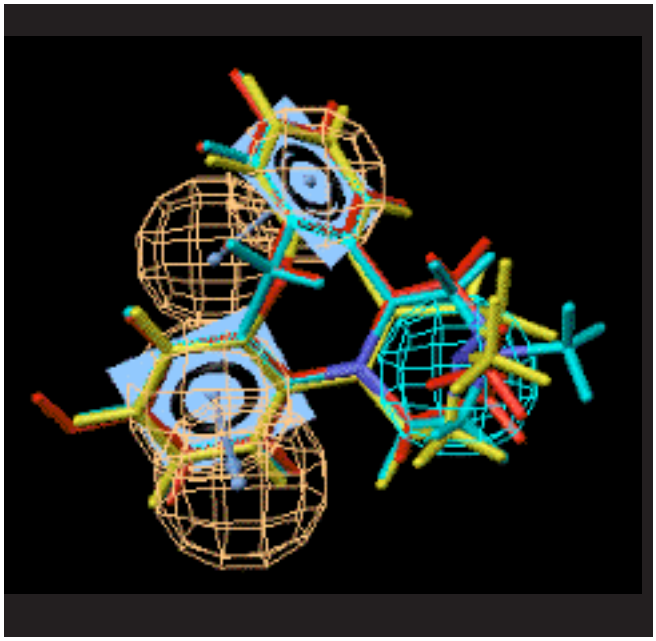

Figure 3b. *Mapping of mianserin (light green), hydroxymianserin (red) and maroxepine (yellow) onto hypotheses* ***3,*** *which consists of hydrophobic (green), ring aromatic 1 (yellow) and ring aromatic 2 (yellow).*

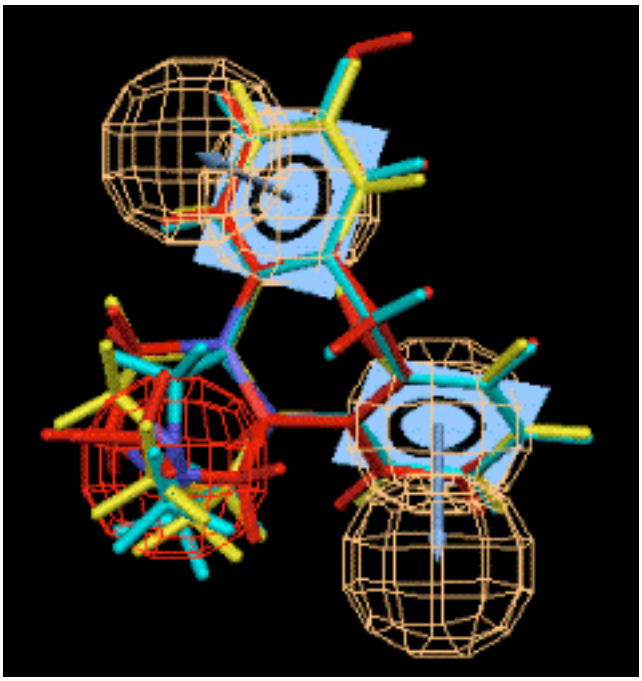

Figure 3c. *Mapping of mianserin (light green), hydroxymianserin (red) and maroxepine (yellow) onto hypotheses* ***9,*** *which is characterized by positive ionizable (red), ring aromatic 1 (yellow) and ring aromatic 2 (yellow) features.*

ity is defined using the minimum description length principle from information theory. The overall cost of a hypothesis is calculated by summing three cost factors: weight cost (a value that increases in a gaussian form as the feature weight in a model deviates from an idealized value of 2.0), error cost (a major value that increase as the RMS (Root Mean Square) difference between estimated and measured activities) and configuration cost (a fixed cost which depends on the complexity of the hypothesis, equal to Entropy of the hypothesis space). Not only a numerical score for each generated hypothesis, Catalyst also provides the cost values of an ideal hypothesis and of the null hypothesis. An ideal hypothesis is a lower bound on the cost of the simplest hypothesis that still fits the data perfectly. Cost of the null hypothesis presumes that there is no statistically significant structure in the data, and that the experimental activities are normally distributed about their mean. Generally, the greater the difference between the two costs, the higher the probability for finding useful models. In terms of hypothesis significance, a generated hypothesis with a score that is substantially below that of the null hypothesis is likely to be statistically significant and bears visual inspection. It's reported that a returned hypothesis which has a cost that differs from the null hypothesis by 40 - 60 bits might possess a 75 - 90 % chance of representing a true correlation. Using the Fisher method [18], the statistical significance of the hypothesis was accessed by randomizingly scrambling the

Table 2. *Predicted activity from 10 best hypotheses against actual binding activity data for 20 antagonists*

Comps.	Exp.	Confs.	Hypo. 1	Hypo. 2	Hypo. 3	Hypo. 4	Hypo. 5	Hypo. 6	Hypo. 7	Hypo. 8	Hypo. 9	Hypo.10
1	1.0	23	3.1	5.3	1.6	2.1	2.3	12	1.1	7.1	11	16
2	1.2	16	2.5	2.6	1.5	2.2	1.3	4.7	3.2	8.4	6.3	8.3
3	1.7	15	3.7	3.2	1.6	3.2	1.7	4.7	1.6	13	10	8.3
4	19.1	101	16	12	52	25	41	15	470	31	26	92
5	35.5	55	24	28	80	43	130	5.9	210	99	62	140
6	55.0	10	1000	1200	710	730	650	1500	570	12	10	8.3
7	117.5	71	98	45	660	740	660	30	800	190	420	130
8	269.2	138	380	400	680	730	700	630	470	3200	3200	3700
9 *	478.6	22	3.1	4.6	1.5	2.5	2.1	7.5	1.2	9.5	8.3	14
10	758.6	54	620	560	800	730	750	170	460	52	150	280
11	851.1	14	1900	1700	790	750	750	1500	480	370	140	88
12	1445.4	62	1200	1200	910	720	810	1500	480	330	430	160
13	1584.9	58	1500	1400	790	720	810	1400	500	3100	3200	3300
14	1819.7	21	1100	1400	800	1300	820	1900	590	3200	3500	3500
15	2884.0	73	1000	850	750	720	660	1200	670	4400	4600	3700
16	3235.9	89	1100	1200	790	710	780	1400	490	560	250	170
17	16982.4	247	1000	1100	1200	960	910	1400	1100	3100	3200	3300
18	29512.1	212	22000	29000	17000	41000	20000	14000	17000	3100	3200	3200
19 *	52480.7	94	18	12	900	820	710	53	650	3100	3330	3300
20 *	81283.1	253	9.5	8.2	660	700	640	8.1	470	3600	3800	3400

** excluded from hypothesis generation. Abbreviations: Comps. compounds (ref. Fig. 1 for structures); Exp. experimental data (*pK_i *in nM); Confs. number of configurations; Hypo. hypothesis.*

bioassay activities in 19 new training sets, and regenerating the hypotheses for each new trial.

The quality of the correlation among the data in the training set is given by the RMS score which was normalized by the log (uncertainty) and the regression constant *r*.

Results and Discussions

The characteristics of the ten lowest cost hypotheses that were obtained are listed in Table 1. The total fixed cost of the run is 66.50 and the cost of the null hypothesis is 124.97. The cost range between best hypothesis **1** and null hypothesis is 46.01, the cost range over the 10 generated hypotheses is 13.08. Hypotheses **1**, **2** and **6** consist of same chemical feature functions as Hp1, Hp 2 and RA. Hypotheses **3**, **4**, **5** and **7** consist of three-feature functions, namely Hp, RA 1 and RA 2. The third group composes of hypotheses **8**, **9** and **10** which are characterized by PI, RA 1 and RA 2 common features. Furthermore, comparing procedure and regression studies show that hypotheses **1**, **3** and **9** are the best models among the three groups and are selected for further evaluation (Figs. 3a-c). Even though hypothesis **9** has a slightly higher RMS than **8** (1.493 and 1.461, respectively), they have nearly no difference in cost values and the correction between experimental and predicted activities is higher in hypothesis **9** (0.885 for hypothesis **9** and 0.864 for hypothesis **8**). The regression lines for hypotheses **1**, **3** and **9** are shown in Fig. 2. Apparently, hypotheses **1** and **3** have higher regression correction than **9** (0.934 for hypothesis **1** and 0.927 for hypothesis **3**), and the RMS indices for hypotheses **1** and **3** are very small as 1.047 and 1.093, respectively. These statistical data suggest that the hypothesis models are likely to reflect good chance of correlation. It's expected that the best hypothesis **1** has at least a chance of 95% in representing true correlation in the data [18]. Thus, the statistical significance of the hypothesis was assessed in a randomization trial in which 19 hypotheses generation experiments were conducted using training set spreadsheets with randomizingly scramble activity data. Among the 190 resulting hypotheses, none had a cost score lower than that of hypothesis **1**, and only one had slightly lower cost scores than hypothesis **3**. Three had slightly

Table 3. *Activity and predicted activity of **AAT**s from Hypothesis **1***

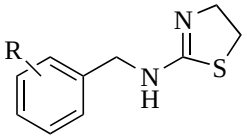

Compound No.	R	Activity (nM)	Predicted Activity	Error
AAT1	H	281.8	410	3.5
AAT2	2-CH_3	645.7	1000	1.5
AAT3	2-Cl	436.5	430	-1
AAT4	2-F	446.7	1000	2.2
AAT5	3-F	251.2	1100	4.5
AAT6	4-F	457.1	1000	2.2
AAT7	2-CF_3	288.4	120	-2.4
AAT8	3-CF_3	380.2	67	-5.7
AAT9	3,4-F_2	446.7	1000	2.3
AAT10	2,5-Cl_2	131.8	110	-1.1
AAT11	2,6-Cl_2	1258.9	510	-2.5
AAT12	2-Cl-4-F	182.0	400	2.2
AAT13	3-Cl-4-F	109.6	1000	3.7

lower cost scores than hypothesis **9**. These tests indicate that the original hypotheses **1**, **3** and **9** represented true correlation in 95, 90 and 80 percent chance, respectively.

All calculated affinity activities from 10 best hypotheses and the number of generated configurations for each molecule are listed in Table 2. Antagonists **9**, **19** and **20** were excluded from the hypothesis generation (see also section 2.1). Mianserin, hydroxymianserin and maroxepine are the three most active compounds, while all hypotheses except hypothesis **7** predicted a little higher affinity for mianserin than that for maroxepine. These molecules map well onto all three hypothesis features at similar way (see Figs. 3a-c) and therefore are considered to be equivalent. This result may also imply that Catalyst treats mianserin-like structures reasonably in the process of calculating a hypothesis. In mapping chlorpromazine which has moderate binding affinity (exp. 758.6 nM) with hypotheses **1**, **3** and **9**, it was found that it mapped two features of these models by RA and Hp. Though the chlorine atom substituted at the hydrophobic benzene ring has the tendency of acting as a hydrophobic block, the distance constraint of chlorine-benzene is found to be between only 2.16-4.17 angstroms in the case of mapping onto hypothesis **1** (Fig. 4). Another reason why chlorpromazine is about 20 times less active than promethazine might contribute to the deviating behaviour in mapping of chlorine-substituted benzene ring with RA. An ideal distance between the two hydrophobic groups is 5.33 angstroms in mianserin-hypothesis **1** model (see Fig. 4). Meanwhile, ideal distances of RA-HB 1 and RA-HB 2 in hypothesis **1** are 4.57 and 4.66 angstroms. It's interesting that promethazine (exp. 35.48 nM), an analogue of chlorpromazine, seems to utilize its lipid side chain to mimick the hydrophobic aromatic ring in mianserin and chlorine atom in the case of chlorpromazine with a proper distance constraint of about 4.58-6.58 angstroms (Fig. 4). The HB function near the Cl group of chlorpromazine is confirmed by the discovery that imipramine (exp. 1445.4 nM), which lacks such a hydrophobic group, is about three times less active than chlorpromazine. Using hypothesis **3** to predict the activity of an outliner metoclopramide, a slightly lower affinity value of 900 nM was gained. Propranolol with low affinity (exp. 29,500 nM) fits only one feature of hypothesis **1** or **3**. More active antagonists map well onto all the features of the hypotheses. On the contrary, inactive compounds lack binding affinity are poorly capable of achieving an energetically favourable conformation shared by the active molecules in order to fit the 3D common feature pharmacophore model.

Thus, valuable models were found in hypotheses **1**, **3** and **9** which facilitated the evaluation of the antagonists and prediction of new compounds or could be served as a searchable key in database searching. Roughly speaking, hypothesis **1** and hypothesis **3** have the good similarity in 3D spatial shape.

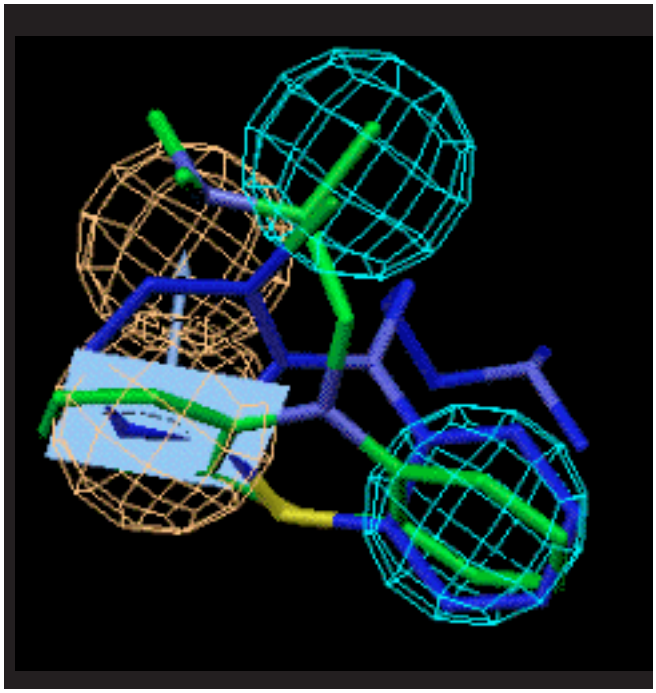

Figure 4. *Mapping of chlorpromazine (blue) and promethazine (green) onto hypothesis **1** (hydrogens on carbons are omitted for clarity). The ideal distance between RA and Hp 2 is 4.66 angstorms, while that of Hp 1-Hp 2 and RA-Hp1 are 5.33 and 4.57 angstroms, respectively. Chlorpromazine maps RA with a slightly deviated benzene ring with its Cl group tending to mimick the hydrophobic 2 feature.*

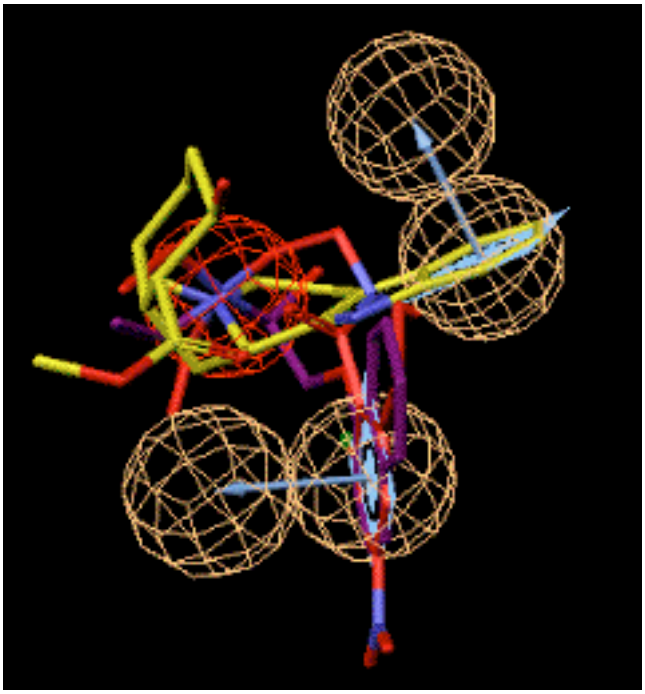

Figure 5. *Mapping of metoclopramide (red, est. 8,000 nM), yohimbine (yellow, est. 29,000 nM) and propranolol (violet, 8,000 nM) onto feature-weight modified hypothesis **9**. Although these molecules can fit the PI feature (red) with a basic amine or amide that is protonated at physiological pH, poor mapping with the two hydrophobic aromatic ring features are observed in this model.*

An aromatic ring feature in hypothesis **3** is considered to be more accurate in assessing mianserin-like compounds which have plural aromatic rings. In spite of a relatively higher RMS and higher cost, hypothesis **9** is important in treating low affinity compounds like propranolol, even including outliners metoclopramide and yohimbine (Fig. 5). Though some of these molecules can fit the PI feature with a basic amine or amide that is protonated at physiological pH, poor mapping with the hydrophobic aromatic ring was observed in this model. Hence, it could be proposed that PI contains a lower feature weight than RA or Hp. Additionally, in a default common hypothesis generation, all chemical features are contributed equally in providing binding energy. This is surely not the right place for most biological systems. Though at most cases, chemists do not know exactly to what extents a common feature interacts with the receptor, it should be useful and challengeable to emphasize some features and to lighten other ones in the process of generating and evaluating a pharmacophore hypothesis. We therefore manually changed the weights of these three feature points, assigning a relative weight of 2 to positive ionizable 1 sphere, a relative weight of 2.5 to the ring aromatic 2 and a higher weight of 3 to the unusual ring aromatic 3. The set of compounds were evaluated again, resulting into high regression correlation. With this feature-weight modified model, yohimbine (exp. 81,200 nM) was found to have an evaluated activity of 29,000 nM, and metoclopramide (exp. 52,500 nM) was predicted to be as inactive as a K_i of 8,000 nM.

The best statistically significant hypothesis **1** was applied to access some synthesized molecules including some 2-(aralkylamino)-2-thiazolines (**AAT**s) [19] whose binding activity was tested against OAR3 on locust. The predicted values and the bioassay activities of these molecules are listed in Table 3. Further calculation on the comparison of the 3D hypotheses from agonists and antagonists are in progress.

Antagonists were studied in generating the hypothesis. The study about the agonists is in progress and will be published in series in the near future. Apparently, antagonists may not interact with the same part of the membrane with which the agonists interact. The ionophore, one component of the cell membrane, may be activated between a ligand-receptor interaction. Antagonists may act via the receptor or via the ionophore or a combination of both. Taken the part of the membrane with which the agonist interacts as the true receptor, the antagonist may well interact with an area surrounding the receptor including the ionophore. Hence, fur-

ther research on the comparison of the 3D hypotheses from agonists and antagonists as well as those generated from the corresponding data from various insect tissues might be interesting and stimulating to investigate further.

Conclusion

Catalyst/Hypo was useful in building 3D pharmacophore models from the binding activity data and conformational structure. It can be used as an alternative for QSAR/QSPR methods preferred with easy visualization and high prediction. Three best hypotheses **1**, **3** and **9** were obtained from this study and were applied to map with the active or inactive compounds. Important features were found in Hp, RA or PI of the surface-assessable models. It was found that for some inactive compounds, their lack of binding affinity is primarily due to their inability to achieve an energetically favourable conformation shared by the active compounds in order to fit the 3D common feature pharmacophore keys. The best statistically significant hypothesis **1** was applied to access some synthesized molecules like **AAT**s, showing a relatively good predictivity.

Based upon this study, several three-dimensional pharmacophore models for the octopamine antagonists-OA3 receptor interactions have been proposed, which are considered to be useful in both searching alternative structural templates from 3D databases and designing new leads for hopefully more active compounds. A comparison study of 3D hypothesis models of antagonists and agonists is in progress and are expected to clarify the mode of action of these compounds acting on OAR3. On the other hand, such work will surely help elucidate the mechanisms of OAR3 and other types of octopamine receptor-ligand interactions.

Acknowledgments: This work was supported in part by a Grant-in-Aid for Scientific Research from the Ministry of Education, Science, and Culture of Japan. The Catalyst program is the property of Molecular Simulations Incorporated, San Diego, CA 92121-3752.

References

1. Hansch, C.; Leo, A. In *Exploring QSAR: Fundamentals and Applications in Chemistry and Biochemisry*; American Chemical Society: Washington, DC, 1995.
2. Hansch, C.; Fujita, T. *J. Am. Chem. Soc.* **1964**, *86*, 1616.
3. Golender, V.E.; Vorpagel, E.R. In *Computer-Assisted Pharmacophore Identification, in 3D-QSAR in Drug Design: Theory, Methods, and Applications;* ESCOM Science: The Netherlands, 1993.
4. Harmar, A. J.; Hom, A. S. *Molec. Pharmac.* **1997**, *13*, 512.
5. Erspamer, V.; Boretti, G. *Arch. Int. Pharmacodyn.* **1951**, *88*, 296.
6. Axelrod, J.; Saavedra, J.M. *Nature* **1977**, *265*, 501.
7. Evans, P.D. In *Octopamine in Comprehensive Insect Physiology Biochemistry Pharmacology*; Pergamon: Oxford, 1985.
8. Saavedra, J.M. *Handb. Exp. Pharmacol.* **1989**, *90*, 181.
9. Orchard, I.; Ramirez, J.M.; Lange, A. B. *Ann. Rev. Entomology* **1993**, *38*, 227.
10. Nathanson, J.A. *Mol. Pharmac.* **1985**, *28*, 254.
11. Evans, P.D. *J. Physiol.* **1981**, *318*, 99.
12. Roeder, T. *Life Science* **1991,** *50*, 21.
13. Roeder, T. *European J. of Pharmac*. **1990**, *191*, 221.
14. Roeder, T. *British J. of Pharmac.* **1995**, *114*, 210.
15. Pan, C.; Hirashima, A.; Tomita, J.; Kuwano, E.; Taniguchi, E.; Eto, M. *Internet J. of Science -Biol. chem.* **1997**, Vol 1 (http://www.sci-journal.com/97v1/).
16. Smellie, A.; Teig, S.L.; Towbin, P. *J. Comp. Chem.* **1995**, *16*, 171.
17. Smellie, A.; Kahn, S. D. Teig, S.L. *J. Chem. Inf. Comp. Sci.* **1995**, *35*, 295.
18. Fisher, R. In: *The Design of Experiments*; Hafner: New York, 1996.
19. Hirashima A.; Tarui H.; Taniguchi E.; Eto M. *Pesticide Biochem. and Physio.* **1994**, *50*, 83.